

Article

Characteristics and Source Apportionment of Volatile Organic Compounds in an Industrial Area at the Zhejiang–Shanghai Boundary, China

Xiang Cao ¹, Jialin Yi ¹, Yuwu Li ², Mengfei Zhao ³, Yusen Duan ², Fei Zhang ⁴  and Lian Duan ^{1,*}

¹ School of Environment and Architecture, University of Shanghai for Science and Technology, Shanghai 200093, China; 213362161@st.usst.edu.cn (X.C.); 2035041026@st.usst.edu.cn (J.Y.)

² Shanghai Environmental Monitoring Center, Shanghai 200235, China; liyw@sthj.shanghai.gov.cn (Y.L.); duanys@yeah.net (Y.D.)

³ Zhejiang Environmental Technology Co., Ltd., Hangzhou 311500, China; zhaomengfei@zjshjkj.com

⁴ College of Environmental and Resource Sciences, Zhejiang University, Hangzhou 310058, China; feizhang@zju.edu.cn

* Correspondence: duanlian@usst.edu.cn

Abstract: As “fuel” for atmospheric photochemical reactions, volatile organic compounds (VOCs) play a key role in the secondary generation of ozone (O₃) and fine particulate matter (PM_{2.5}, an aerodynamic diameter ≤ 2.5 μm). To determine the characteristics of VOCs in a high-level ozone period, comprehensive monitoring of O₃ and its precursors (VOCs and NO_x) was continuously conducted in an industrial area in Shanghai from 18 August to 30 September 2021. During the observation period, the average concentration of VOCs was 47.33 ppb, and alkanes (19.64 ppb) accounted for the highest proportion of TVOCs, followed by oxygenated volatile organic compounds (OVOCs) (13.61 ppb), alkenes (6.92 ppb), aromatics (4.65 ppb), halogenated hydrocarbons (1.60 ppb), and alkynes (0.91 ppb). Alkenes were the predominant components that contributed to the ozone formation potential (OFP), while aromatics such as xylene, toluene, and ethylbenzene contributed the most to the secondary organic aerosol production potential (SOAFP). During the study period, O₃, NO_x, and VOCs showed significant diurnal variations. Industrial processes were the main source of VOCs, and the second largest source of VOCs was vehicle exhaust. While the largest contribution to OFP was from vehicle exhaust, the second largest contribution was from liquid petroleum gas (LPG). High potential source contribution function (PSCF) values were observed in western and southeastern areas near the sampling sites. The results of a health risk evaluation showed that the Hazard Index was less than 1 and there was no non-carcinogenic risk, but 1,3-butadiene, benzene, chloroform, 1,2-dibromoethane, and carbon tetrachloride pose a potential carcinogenic risk to the population.

Keywords: volatile organic compounds; diurnal variation; OFP; SOAFP; source apportionment; health risk assessment



Citation: Cao, X.; Yi, J.; Li, Y.; Zhao, M.; Duan, Y.; Zhang, F.; Duan, L.

Characteristics and Source Apportionment of Volatile Organic Compounds in an Industrial Area at the Zhejiang–Shanghai Boundary, China. *Atmosphere* **2024**, *15*, 237. <https://doi.org/10.3390/atmos15020237>

Academic Editor: Kumar Vikrant

Received: 22 January 2024

Revised: 10 February 2024

Accepted: 15 February 2024

Published: 18 February 2024



Copyright: © 2024 by the authors. Licensee MDPI, Basel, Switzerland. This article is an open access article distributed under the terms and conditions of the Creative Commons Attribution (CC BY) license (<https://creativecommons.org/licenses/by/4.0/>).

1. Introduction

With the continuous increase in energy consumption resulting from the acceleration of urbanization and industrialization, air pollution, represented by ozone (O₃) and fine particulate matter (PM_{2.5}, an aerodynamic diameter ≤ 2.5 μm), has become an increasingly serious atmospheric problem [1–3]. Volatile organic compounds (VOCs), as “fuel” for atmospheric photochemical reactions, play a key role in the secondary generation of O₃ and PM_{2.5} [4]. The chemical composition of VOCs in the ambient atmosphere is complex and mainly includes non-methane hydrocarbons (NMHCs), oxygenated volatile organic compounds (OVOCs), halogenated hydrocarbons, nitrogen-containing organic compounds, and sulfur-containing organic compounds. Carbonyl compounds, including aldehydes and ketones, have an important influence on the reactive radical cycle and secondary pollutant generation [5].

In recent years, high-level urban and regional O₃ pollution episodes have been frequent in China. As the primary precursor of ozone pollution, many studies on VOCs have been conducted to provide ideas for urban and regional O₃ prevention and control. Yu et al. [6] found that the proportion of vehicle emissions and liquid petroleum gas/natural gas (LPG/NG) contribution increased year by year, while the proportion of industrial and solvent sources showed a decreasing trend. Li et al. [7] found that VOCs in suburban areas are mainly from traffic in urban areas and that urban sites are very active in photochemical processes. The same study in Beijing showed a significant decrease in average VOC concentrations in 2018 compared to 2015 and 2016, with regional transport mainly from the south–southeast (SSE) and south–southwest (SSW) and a tendency toward a transitional state of O₃ sensitivity in the summer. Strong solar radiation, a high temperature, and low humidity exacerbate O₃ pollution, which is further exacerbated by regional transport from polluted areas in the south [8]. Tan and Wang [9] reviewed VOC characteristics during a Shanghai citywide closure period, showed that reductions in O₃ precursors and other pollutants did not prevent ground-level O₃ pollution during the 2022 closure period; high O₃ concentrations were primarily due to large reductions in nitrogen oxide (NO_x) emissions, while reductions in volatile organic compound (VOC) concentrations could not overcome the titration effect of nitric oxide (NO). A study of air pollution in the Dongguan industrial area during the COVID-19 lockdown showed that the average concentrations of NO_x and VOCs decreased compared to the pre-lockdown period. In contrast, the average ozone concentration increased slightly; the analysis concluded that the increase in ozone was the combined result of a large increase at night and a small decrease during the day [10]. VOCs may adversely affect public health (e.g., respiratory and cardiovascular systems) at certain concentrations. Previous studies found significant positive correlations between personal exposures and VOC concentrations and greater risk-of-hazard quotients and cancer in areas of high VOC exposure [11,12]. As a result, toxic VOCs like benzene are classified as hazardous air pollutants by the United States Environment Protection Agency (USEPA).

In Shanghai, rapid urbanization and industrialization make VOC pollution more serious than ever before. Numerous studies have been conducted to analyze the characteristics of VOCs in Shanghai in recent years [13–16]. However, these studies have focused more on the overall characteristics of VOCs in Shanghai, and relatively few studies have been conducted in each district. Jinshan District, where many of Shanghai's industrial parks are located, has attracted less attention. Therefore, it is necessary to measure and understand the characteristics of VOCs in Jinshan District.

In this study, 113 VOCs, O₃, and NO_x at provincial boundary sites in Jinshan were monitored from August to September 2021 to carry out atmospheric VOC characteristics, diurnal variations, ozone and secondary organic aerosol formation potential determinations, and a source analysis. The results will be helpful to better understand ozone and secondary organic aerosol (SOA) pollution and the formation mechanism in this region, which can provide technical support for the development of regional air pollution control countermeasures.

2. Materials and Methods

2.1. Observation Overview

In this study, a GC3000-MS produced by Spectrum Technology was used to measure high-carbon VOC species from C₆ to C₁₀, and a GC3000-315L was used to determine low-carbon VOC species from C₂ to C₅. VOCs were monitored from 18 August to 30 September 2021 at provincial boundary station (121.27° N, 30.71° E) which is located in a large integrated industrial area in Jinshan District, in the southwest of Shanghai (as shown Figure 1). There are multiple paint companies within a 3 km radius of the station which use large amounts of solvents in their production processes. There is a large chemical zone to the northeast of the site, with several Sinopec gas stations and petrochemical companies in the vicinity. In total, 113 VOCs, including 29 alkanes, 11 alkenes, 17 aromatic hydrocarbons, 35 halogenated hydrocarbons, 20 oxygenated organic compounds (OVOCs), and acetylene,

were monitored online using a gas chromatography–mass selective detector/flame ionization detector (GC-MSD/FID, Puyu Technology Development Co., Ltd., Hangzhou, China). The time resolution was 1 h. The sampling system collects ambient air in two channels. The samples of the two channels were dehydrated and enriched by a low-temperature pretreatment system, and the gas samples were quickly transported to a capillary column for subsequent separation by direct thermal desorption at a high temperature. The separated volatile organic compounds were detected by MS and FID detectors, and qualitative and quantitative analysis results were obtained through data processing. Details can be found in a previous study [17]. Synchronized observations of pollutants, O₃, NO₂ and meteorological parameters (temperature, humidity, wind speed, and direction) were carried out at the site. Statistical analyses were conducted using the Origin software. During the observation period, the average temperature was 27.2 °C, varying between 20.3 °C and 33 °C, the relative humidity ranged between 50% and 100% with an average of 94.3%, and the mean wind speed was 2.9 m/s during the observation period.

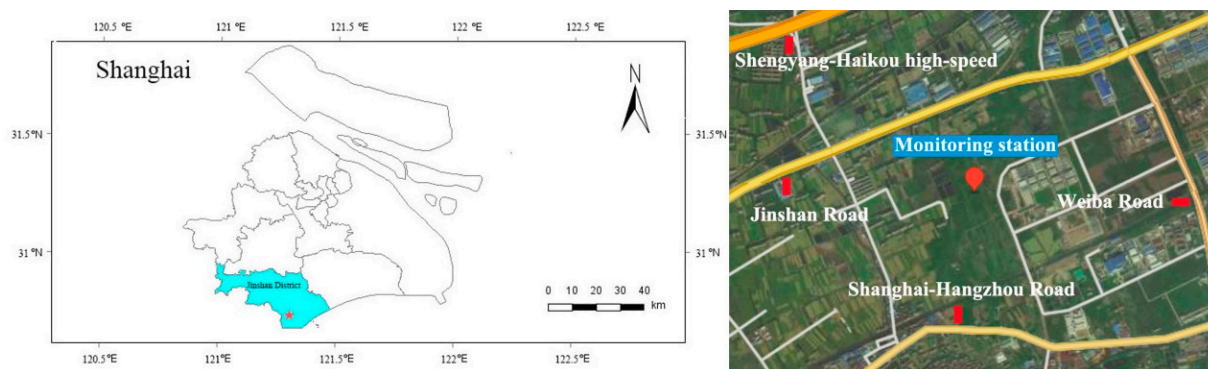


Figure 1. Satellite imagery showing the sampling site and surrounding area.

2.2. Ozone Formation Potential (OFP)

Various species of VOCs in the atmosphere have different concentration levels and reactive activities. The contribution to ozone formation varies greatly. Currently, the ozone formation potential (OFP) is commonly used to assess the potential contribution of VOCs to ozone formation. The calculation formula is as follows:

$$\text{OFP}_i = [\text{VOCs}]_i \times \text{MIR}_i, \quad (1)$$

where OFP_i is the ozone formation potential of the VOC species i ($\mu\text{g}/\text{m}^3$); $[\text{VOCs}]_i$ is the average concentration of the VOCs species i ($\mu\text{g}/\text{m}^3$); MIR is the maximum incremental reactivity of the VOC species i . MIR is referenced from Carter's study [18].

2.3. Secondary Organic Aerosol Formation Potential (SOAFP)

In this study, the contribution of various VOCs to the generation of secondary organic aerosols was assessed using the secondary organic aerosol formation potential (SOAFP) based on the Grosjean smoke box experiment with the following formula [19,20]:

$$\text{SOAFP}_i = [\text{VOCs}]_i \times \text{FAC}_i, \quad (2)$$

where SOAFP_i is the secondary organic aerosol formation potential of the VOC species i ($\mu\text{g}/\text{m}^3$); $[\text{VOCs}]_i$ is the average concentration of the VOCs species i ($\mu\text{g}/\text{m}^3$); and FAC_i is the aerosol generation coefficient for a species i . The values are taken with reference to Grosjean et al. [19,20].

2.4. Potential Source Contribution Function (PSCF)

The PSCF is an analysis method based on trajectory and pollutant concentration to identify potential pollution source areas [21–23]. Its analysis is run by TrajStat, which is a GIS-based software that uses different trajectory statistical analysis techniques (e.g., HYSPLIT) to identify potential sources of atmospheric pollutants [21,24]. It has been extensively used in previous studies [25]. The PSCF value can determine the proportion of pollution tracks in the grid. The PSCF is defined as

$$\text{PSCF}_{ij} = \frac{m_{ij}}{n_{ij}}, \quad (3)$$

where i is the latitude, j is the longitude, n_{ij} is the number of endpoints falling in the ij cell, and m_{ij} is the number of “polluted” trajectory falling in the cells. In this study, the average mixing ratio of VOCs is used as the pollution threshold. In order to reduce the influence of small n_{ij} values, it is necessary to multiply any weight function $W(n_{ij})$ by the PSCF value to better reflect the uncertainty in cells [26,27]. The weight function is defined as follows:

$$\text{WPSCF}_{ij} = \frac{m_{ij}}{n_{ij}} \times W(n_{ij}), \quad (4)$$

$$W(n_{ij}) = \begin{cases} 1.00, & 80 < n_{ij} \\ 0.72, & 20 < n_{ij} \leq 80 \\ 0.42, & 10 < n_{ij} \leq 20 \\ 0.05, & n_{ij} \leq 10 \end{cases}, \quad (5)$$

2.5. Positive Matrix Factorization (PMF) Model

The source apportionment of VOCs was performed using the PMF model [23]. PMF is a receptor model for the source identification of atmospheric pollutants. PMF has been widely used for source analyses of VOCs, and its principle and applications have been detailed in many papers [28,29]. Here, for VOC species with concentrations equal to or less than the method detection limit (MDL), the uncertainty is set to 5/6 of the MDL (Equation (6)). And for species with concentrations higher than the MDL, the uncertainty is defined as in Equation (7).

$$\text{Unc} = \frac{5}{6} \times \text{MDL} \quad (x_i \leq \text{MDL}), \quad (6)$$

$$\text{Unc} = \sqrt{(\text{Error Fraction} \times x_i)^2 + (0.5 \times \text{MDL})^2} \quad (x_i > \text{MDL}), \quad (7)$$

where Unc is the uncertainty of a VOC species i , and x_i is the concentration of species i . In this study, the MDL is uniformly taken as 0.05. The method of calculating the Error Fraction is as follows: first, find out the standard deviation and mean value of x_i , and finally, express the Error Fraction as a relative standard deviation of x_i . In this study, a total of 46 representative VOCs with complete data were used for the source analysis.

2.6. Health Risk Assessment

A health risk evaluation quantifies the risk of pollutants causing harm to the health of the population, using the risk level as the evaluation index. Based on the carcinogenicity of the pollutants, which can be categorized into carcinogenic risk and non-carcinogenic risk, the carcinogenicity of VOCs is evaluated using the HI (Hazard Index) and Risk (Lifetime Cancer Risk) [30]. The calculation formulae are as follows:

$$\text{EC} = (\text{CA} \times \text{ET} \times \text{EF} \times \text{ED}) / \text{AT}, \quad (8)$$

$$\text{HQ} = \text{EC} / (\text{RfC} \times 1000), \quad (9)$$

$$HI = \sum HQ_i, \quad (10)$$

$$\text{Risk} = EC \times IUR, \quad (11)$$

where EC is the exposure concentration ($\mu\text{g}/\text{m}^3$); CA is the concentration of the VOC species i ($\mu\text{g}/\text{m}^3$); ET is the exposure time, 24 h/d; EF is the exposure frequency, 365 d/a; ED is the lifetime exposure time, 80 a; AT is the averaging time, $80 \times 365 \times 24$ h; IUR is the risk per unit of inhalation ($\mu\text{g}/\text{m}^3$); and RfC is the reference concentration (mg/m^3); The values of IUR and RfC can be found in EPA's Integrated Risk Information System (IRIS, <http://www.epa.gov/iris>, accessed on 10 December 2023). It is generally recognized that a non-carcinogenic risk exists when $HI > 1$ and a carcinogenic risk exists when $\text{Risk} > 10^{-6}$ [31].

3. Results and Discussion

3.1. VOC Pollution Levels

3.1.1. General Characteristics Data Overview

Time series of meteorological parameters and pollutants during the observation period are shown in Figure 2. Based on the National Ambient Air Quality Standard (GB 3095-2012), a day with hourly ozone concentration exceeding the Grade II limit value of $200 \mu\text{g}/\text{m}^3$ is defined as an ozone-polluted day. According to the guideline, 18 August, 22 August, 26 August, 28 August, 1 September, 2 September, 6 September, 21 September, and 22 September were classified as polluted days. Notably, the hourly ozone concentration at 15:00 on September 1 reached the highest value of $291 \mu\text{g}/\text{m}^3$ during the period of pollution, and the concentrations at 14:00 and 17:00 on that day were the second and third highest. During the observation period, the mean VOC concentration was 47.33 ppb, which was higher than other studies in Nanjing (34.4 ppb) [32], Chongqing (24.0 ppb) [33], and Zhengzhou (28.8 ppb) [34]. The results of this study are comparable with results in Tokyo (43.3 ppb) [35]. The reasons for the differences in concentrations may be related to meteorological conditions, boundary layer height, and local control policies in different cities. In this study, VOC species are in the following order: alkanes > OVOCs > alkenes > aromatic hydrocarbons > halogenated hydrocarbons > acetylene. Their average concentrations were 19.64 ppb, 13.61 ppb, 6.92 ppb, 4.65 ppb, 1.60 ppb, and 0.91 ppb, respectively (the order of VOC species on polluted and non-polluted days was the same). This result was similar to previous study conducted in the Second Jinshan Industrial Area in Shanghai [36] In Shenzhen, the order is alkanes > OVOCs > halogenated hydrocarbons > aromatics > alkenes > acetylene > acetonitrile [33]. Among them, the concentration of alkanes is much higher than the concentrations of the other VOCs. It is noteworthy that on individual days, there is also a steep increase in the concentration of alkenes.

The diurnal variations in meteorological parameters for polluted and non-polluted days are illustrated in Figure 3. The temperature was always higher on polluted days than on non-polluted days; high temperatures favor photochemical reactions, and more ozone is produced. Similarly, the wind speed was always lower on polluted days than on non-polluted days, and a lower wind speed means more accumulation of pollutants. Except for the period from 19:00 to 05:00, the humidity was lower on polluted days than on non-polluted days, and low humidity weakens the wet removal of ozone, which also affects the concentration of ozone [37]. In summary, the meteorological conditions on polluted days were more favorable for the accumulation of pollutants and for the production and accumulation of ozone.

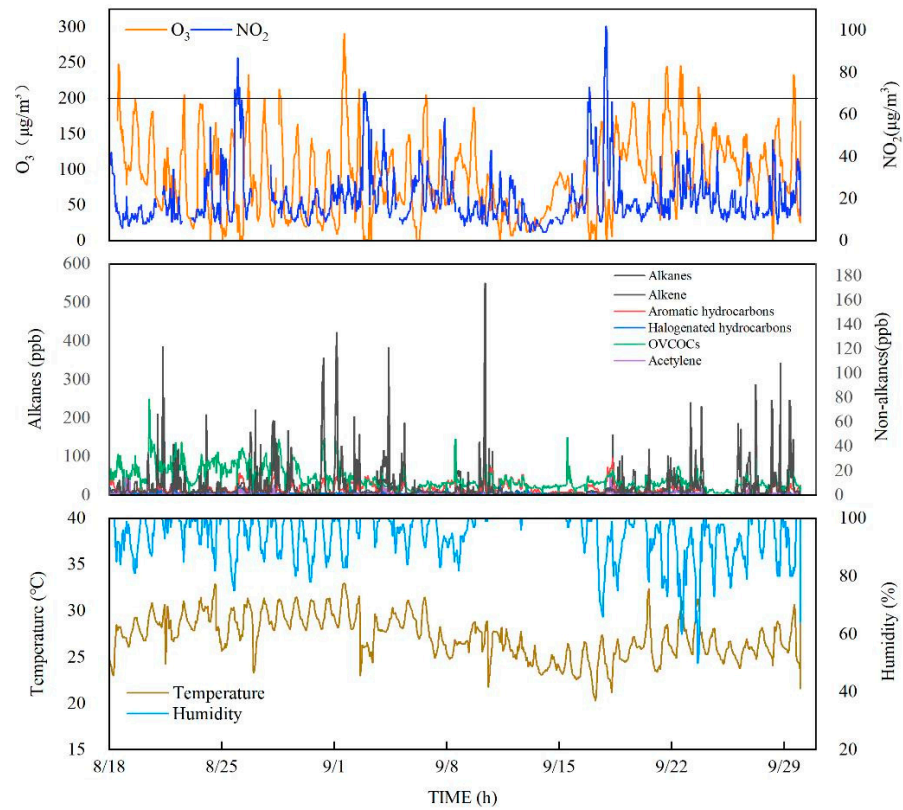


Figure 2. Time series of meteorological parameters and pollutants during the observation period. The black solid line in the graph of daily ozone change indicates an ozone concentration of $200 \mu\text{g}/\text{m}^3$.

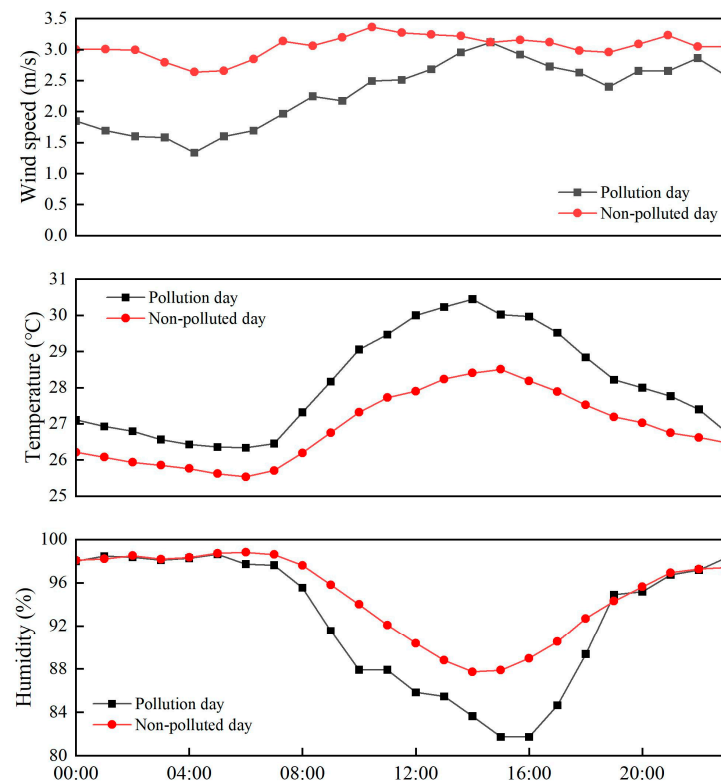


Figure 3. Characteristics of diurnal variations in meteorological parameters on polluted and non-polluted days.

3.1.2. Analysis of OFP and SOAFP for VOCs

The concentration, OFP, and SOAFP of the top 15 VOCs during the observation period are shown in Figure 4. The sum of the concentration of the top 15 VOCs was 35.16 ppb, accounting for 74.2% of the total VOCs. Isopentane, propane, propionaldehyde, n-butane, and ethylene are the top five in order of concentration, which indicates that these substances contribute a high proportion of the local VOC concentration. In Figure 4b, the total OFP of the 15 VOCs was 291 $\mu\text{g}/\text{m}^3$. Among these VOCs, OVOCs such as propionaldehyde, acetone, and acetaldehyde are not only associated with primary emissions but also with secondary photochemical generation. Alkenes such as ethylene and propylene dominate the ozone generation potential due to their own higher concentrations and high MIR values. This indicates that it is necessary to pay attention not only to VOCs with high concentration values but also to those VOCs with low concentration values but a strong influence on air pollution. Ethylene is widely used in industrial development [38], and its concentration was high because the observation site is located in an industrial area. Isoprene is an indicator of biogenic emissions and is emitted from many plants [39,40]. The C2-C5 hydrocarbon species are the main components of fossil fuels [41] due to the high volume of traffic and the presence of a large number of factories with strong industrial activity in the vicinity.

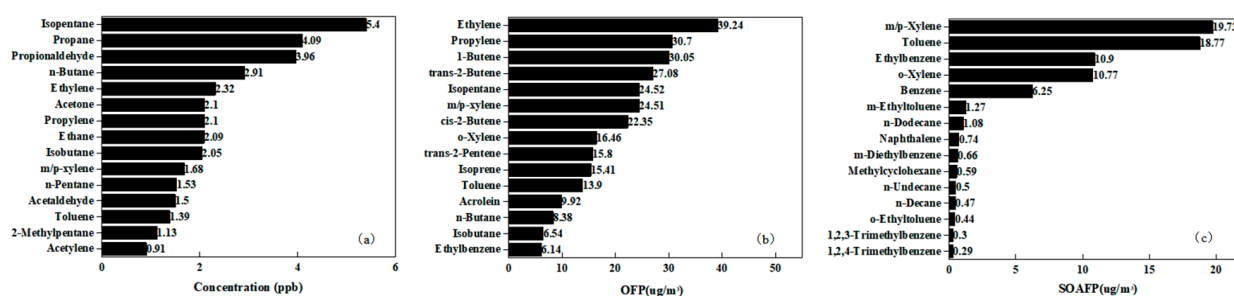


Figure 4. VOCs ranked in the top 15 in terms of (a) concentration, (b) the OFP, and (c) the SOAFP.

The largest contribution to the SOAFP was m/p-xylene ($19.72 \mu\text{g}/\text{m}^3$, 26.6%), followed by toluene ($18.77 \mu\text{g}/\text{m}^3$, 25.3%) and ethylbenzene ($10.90 \mu\text{g}/\text{m}^3$, 14.7%). Among the 15 VOCs that contribute the most to the SOAFP, 11 of them are aromatic hydrocarbons, accounting for the largest proportion (over 90%), which is consistent with the research results of Li et al. [42]. Most of the aromatic hydrocarbons, such as toluene, ethylbenzene, and xylene, come from the use of coating solvents, so strengthening control over the coating solvent industry is essential for reducing the local SOA concentration.

3.2. Diurnal Variations

The diurnal variation characteristics of different air pollutants are shown in Figure 5. The ozone concentration was lower and decreased faster on polluted days than on non-polluted days before 08:00. Meteorological conditions on polluted days were more conducive to the accumulation of pollutants than on non-polluted days, resulting in a stronger titration effect. Ozone concentration increased at a faster rate after 08:00, reaching a maximum concentration ($205.46 \mu\text{g}/\text{m}^3$) at 15:00. Higher temperatures, lower wind speeds, and lower humidity on pollution days made ozone generation and accumulation easier. After 15:00, ozone concentrations started to decrease; this occurred more rapidly on pollution days than on non-pollution days due to the fact that more VOCs accumulated on polluted days and depleted ozone more rapidly.

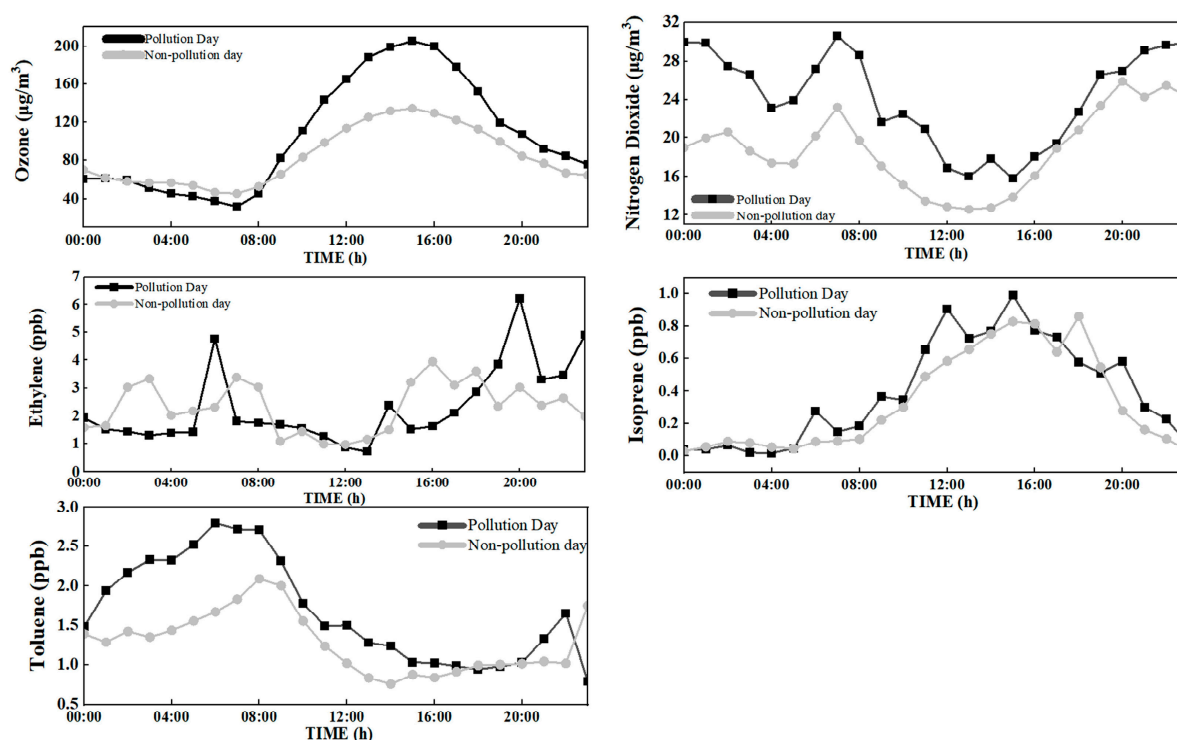


Figure 5. Diurnal variation characteristics of ozone, nitrogen dioxide, ethylene, isoprene and toluene on polluted and non-polluted days.

The diurnal concentration of nitrogen dioxide was characterized by a “double peak and a valley”, maintaining a high concentration during the night, decreasing around 02:00 and reaching a minimum around 04:00 due to the titration effect in the early morning. Due to boundary layer uplift and the depletion of photochemical reactions [43], the concentration reached its first peak at 07:00 and then started to decrease rapidly. On polluted days, there were occasional increases in NO_2 concentrations, suggesting an additional source of NO_2 production during this period. The concentration dropped to a minimum at 15:00, when the ozone concentration also reached a maximum. Thereafter, the concentration of nitrogen dioxide rose again due to the beginning of the evening rush hour, increased traffic flow, and reduced light radiation, resulting in weaker photochemical reactions. Finally, the concentrations equalized at night.

The diurnal variation in ethylene concentration also roughly showed the characteristics of “two peaks and one valley”. The concentration started to rise around 05:00, reached a peak, and then was consumed by the reaction; the concentration started to fall and then rose again in the evening peak. Compared with non-polluted days, the second peak was reached later on polluted days, and the concentration tended to then stabilize.

For isoprene, the polluted days displayed a similar pattern to the non-polluted days, both of which were single-peaked. The concentration was the lowest at night and started to increase after early morning, peaked around 15:00, and then started to decrease. The concentrations on polluted days were slightly higher than on non-polluted days because the high temperature makes plants emit more isoprene [44], and the low wind speed also facilitates the accumulation of isoprene.

Toluene showed the same diurnal pattern on polluted and non-polluted days, with the highest maximum concentration on polluted days peaking earlier than on non-polluted days. The concentration of toluene gradually increased at night and peaked around 08:00, after which the concentration started to decrease at a faster rate. After reaching a minimum around 15:00, the concentration remained at a relatively stable level.

3.3. Source Analysis

3.3.1. Identification of PMF Factors

Variation in the mixing ratio of VOCs during the sampling period may be due to changes in the contribution of emission sources. Ratios of specific VOCs are commonly used to identify emission sources. In this study, the reaction rates of n-butane and isobutane with OH radicals are similar, while the difference in their ratios is less than 10%, which indicates that they are from different sources. Butane is usually from natural gas, LPG, vehicle emissions, and biomass combustion, and the isobutane/n-butane ratios of different sources are different (e.g., 0.2–0.3 for vehicles, 0.46 for LPG, and 0.6–1.0 for NG) [45,46]. In this study, n-butane and isobutane showed a highly significant correlation ($R^2 = 0.882 > 0.6$), indicating that the sources of these two species are similar. The ratio of n-butane/isobutane was 0.54, indicating that the source of n-butane and isobutane emissions was LPG.

N-pentane and isopentane have similar atmospheric lifetimes; thus, the ratio of n-pentane to isopentane is widely used to determine the effects of vehicle emissions and combustion emissions, with values varying with sources (e.g., 0.56–0.80 for coal combustion, 1.5–3.0 for liquid gasoline, and 2.2–3.8 for vehicle exhaust) [36,47]. In this study, n-pentane and isopentane did not show a more significant correlation ($R^2 = 0.218 < 0.6$), indicating that the two substances were from different sources.

The emission sources of m/p-xylene and ethylbenzene are similar, but the former is three times more reactive to OH radicals than the latter [48,49]. Therefore, a lower X/E ratio usually indicates more pronounced aging of the gas mass, that is to say, a greater influence of external transport. In this study, the correlations between m,p-xylene and ethylbenzene on non-polluted days ($R^2 = 0.8046$) and on polluted days ($R^2 = 0.7886$) were significant. In particular, the X/E ratio was 2.44 on a polluted day compared to 3.41 on a non-polluted day. This indicates that the external transport influence was greater on the polluted day compared to the non-polluted day.

Compared to specific VOC proportion analyses, a PMF analysis allows for the quantitative determination of VOC source contributions [50]. In this study, six major factors were identified, including solvent usage, surface coatings, industrial processes, vehicle exhaust, combustion emissions, and liquefied petroleum gas (LPG) usage (as shown in Figure 6).

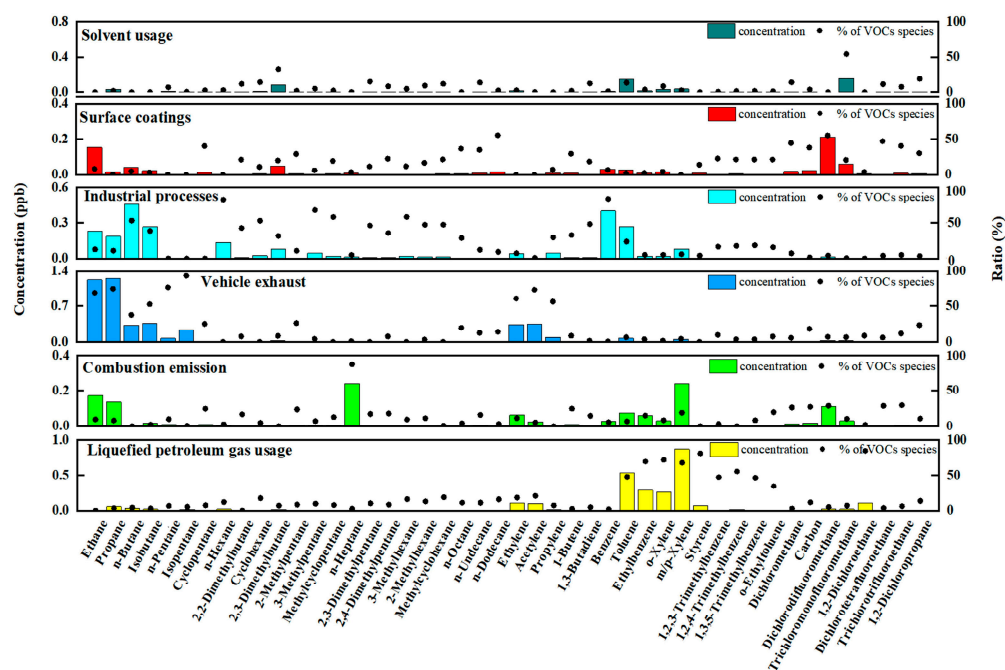


Figure 6. Source profiles and contributions of VOCs.

Factor 1 was mainly characterized by a few short-chain alkanes, and n-hexane, methylcyclopentane, 2-methylpentane-3-methylpentane, and 2,3-dimethylbutane, which are C6-C8 alkanes. Aromatic hydrocarbons such as toluene, xylene, and ethylbenzene made high contributions. The proportions of halogenated hydrocarbons such as carbon tetrachloride and dichloromethane were high. All of these substances are important organic solvents and typical tracers of solvent usage [51,52]. Therefore, factor 1 was highly related to solvent usage.

Factor 2 contained C6-C8 alkanes and a high fraction of aromatic hydrocarbons. Paints usually contain these components [51,53]. Among them, 1,2,3-trimethylbenzene (22.9%), 1,2,4-trimethylbenzene (21.6%) and 1,3,5-trimethylbenzene (21.6%) contributed more. Trimethylbenzene is widely used in coatings [50]. Therefore, factor 2 was identified as surface coatings.

Factor 3 was rich in aromatic and halogenated hydrocarbons. There were large contributions to benzene (83.8%) and toluene (23.6%), which are mainly used in industrial solvent production [54]. Chlorotrifluoromethane, methylene chloride, and 1,2-dichloropropane were shown in previous studies to be associated with industrial processes [26,36]. Ethylene, which is the blood of industrial development [38,55], is also present. Factor 3 also contained long-chain alkanes, of which n-undecane is widely used in industry [32,39]. Thus, we considered this factor an industrial process.

Factor 4 consisted of a high percentage of short-chain alkanes, alkenes, and a small amount of aromatic hydrocarbons. Among them, ethane (69.1%), propane (74.8%), n-butane (37.8%), isobutane (52.6%), n-pentane (76.8%), isopentane (93.6%), ethane (60.8%), and acetylene (73.5%) were particularly prominent. All of these substances are important tracers of automobile exhaust gases [22,51,54,56]. Therefore, factor 4 was defined as vehicle exhaust.

Factor 5 comprised ethane, propane, ethylene, acetylene, and benzene. Acetylene is a typical tracer of combustion emissions [50]. The characteristic combustion products of coal are propane, ethylene, acetylene, and benzene [54]. Ethane is also associated with the use of natural gas [57]. Therefore, factor 5 was apportioned as combustion emissions.

Alkanes (propane, n-butane, and isobutane) and alkenes (ethylene, propylene, and butene) were identified as factor 6, and the use of LPG may release large amounts of short linear alkanes [3]. Combining the previous ratio of n-butane and isobutane, this factor was thus proposed to be LPG.

Based on the results of the source apportionment, the proportion of each VOC source and its OFP were calculated during the observation period (as shown in Figure 7). The largest source of VOCs was industrial processes (36.62%), which is due to the fact that the monitoring site is located near an industrial park and is therefore most influenced by industrial activities. The second source was vehicle exhaust (31.56%), which is related to the high traffic volume in the vicinity. The contribution of LPG usage, which is used more frequently by the locals due to its popularity, was third (15.45%). In contrast, the contributions from surface coatings (3.91%), combustion emissions (8.11%), and solvent usage (4.35%) were relatively small. While in Zhengzhou [58], vehicle exhaust provided a greater contribution (28%), and industrial processes had a lower proportion (28%). Compared to Beijing, the contribution of vehicle exhaust (39.95%) is significant, with natural gas/LPG (22.04%) making the second largest contribution and industrial processes (20.64%) making a relatively low contribution [8]. In terms of OFP, vehicle exhaust made the largest contribution (38.2%), followed by LPG (24%), while industrial processes rank third with a large concentration contribution (17.3%). On the contrary, combustion emissions (10.2%), surface coatings (7.1%), and solvent usage (3.2%) contributed less. Compared to the results of the Zhengzhou study, the contributions of vehicle emissions and industrial processes were significant, but the contribution of solvent usage in this study was not as significant as in Zhengzhou. Due to the high source and OFP contributions from vehicle emissions, reducing vehicle exhaust would be a very effective measure.

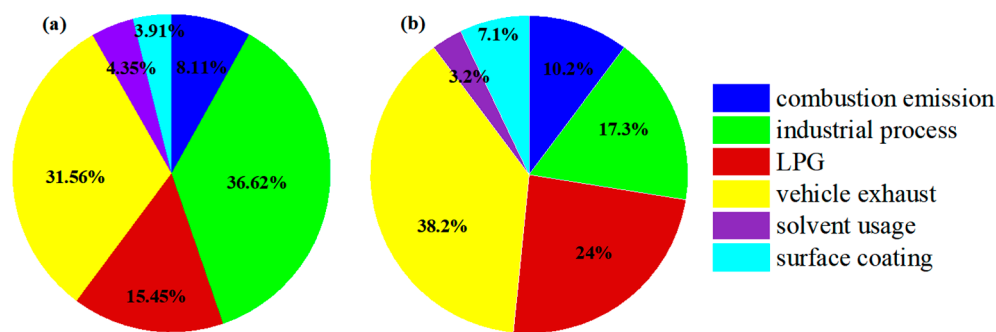


Figure 7. Contribution of each emission source to (a) VOCs and (b) OFP.

3.3.2. The PSCF Results

In addition to the direct impact of local pollution sources, regional transport can also have an impact on VOC pollution. Areas with high PSCF levels indicate high-potential regional transport sources [51]. The results of the PSCF analysis are shown in Figure 8. The highest PSCF values for O₃ in August were mainly distributed in the west and south of the observation site; the highest PSCF values for NO₂ were mainly distributed in the west and southeast, and the TVOCs with the highest PSCF values were mainly distributed in the west. In September, the highest PSCF values for O₃ were mainly distributed in the north and southeast, the highest PSCF values for NO₂ were mainly distributed in the northwest and southeast, and the highest PSCF values for TVOCs were mainly distributed in the southeast. As a result, the potential source areas of pollutants in August were primarily in the west of the site, and the potential source areas in September were the southeast of the site. Again, the role of local pollution sources cannot be ignored.

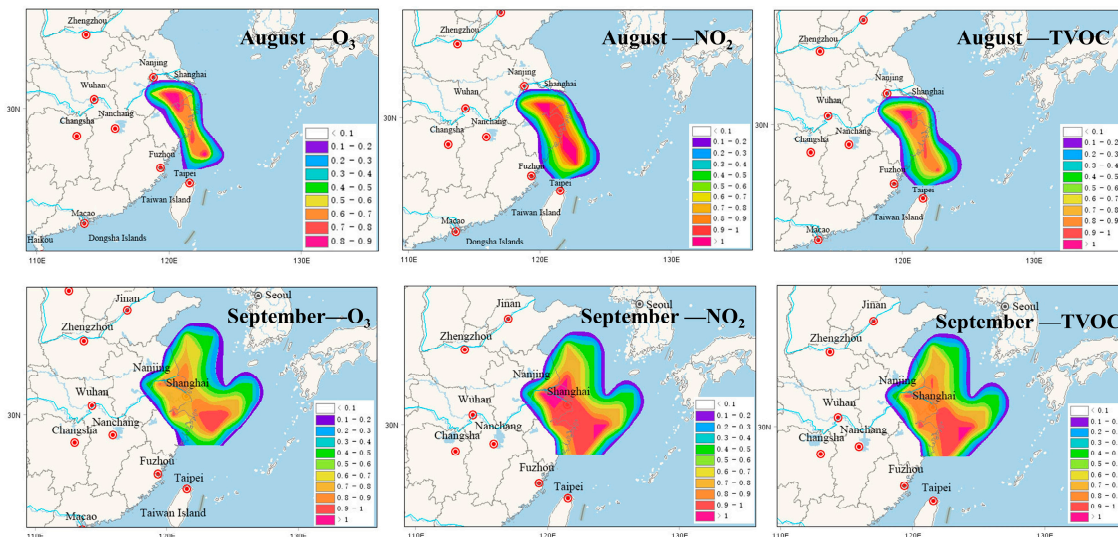


Figure 8. PSCF analysis of O₃, NO₂, and TVOC.

3.4. Health Risk Assessment

Tables 1 and 2 list the calculated non-carcinogenic and carcinogenic risk values for the VOC species available in the EPA Integrated Risk Information System (IRIS) library. According to the risk assessment, an HI value less than 1 indicates that there was no non-carcinogenic risk. In this study, the carcinogenic risk values of 1,3-Butadiene, Benzene, Chloroform, 1,2-Dibromoethane, and Carbon tetrachloride were higher than 10⁻⁶, indicating that these substances have a potential carcinogenic risk. Among them, benzene had the highest lifetime cancer risk value of 7.80 × 10⁻⁶, which was higher than the risk of 2.30 × 10⁻⁶ obtained in a study conducted in Beijing [12]. It was also higher than the

carcinogenic risk of 2.18×10^{-5} in Tianjin [59]. This result may be attributed to the fact that there are a large number of paint solvent companies around this site and the petrochemical industry is booming, both of which are important benzene sources. Therefore, benzene needs to be given sufficient attention to reduce the risk of cancer.

Table 1. Carcinogenic risk assessment of 11 VOCs.

VOC Species	IUR	Risk
1,3-Butadiene	3.00×10^{-5}	1.26×10^{-5}
Benzene	7.80×10^{-6}	2.44×10^{-5}
Vinylchloride	8.80×10^{-6}	9.73×10^{-7}
1,4-Dioxane	5.00×10^{-6}	4.32×10^{-7}
Trichloroethene	4.10×10^{-6}	2.91×10^{-7}
Dichloromethane	1.00×10^{-8}	2.73×10^{-9}
Chloroform	2.30×10^{-5}	5.88×10^{-6}
Tetrachloroethylene	2.60×10^{-7}	3.27×10^{-8}
1,2-Dibromoethane	6.00×10^{-4}	5.07×10^{-6}
Carbon tetrachloride	6.00×10^{-6}	4.41×10^{-6}
Bromoform	1.10×10^{-6}	1.40×10^{-8}

Table 2. Non-carcinogenic risk assessment of 26 VOCs.

VOC Species	Rfc	HQ
m&p-Xylenes	1.00×10^{-1}	4.20×10^{-2}
o-Xylene	1.00×10^{-1}	2.15×10^{-2}
Toluene	5.00×10^0	6.95×10^{-4}
Ethylbenzene	1.00×10^0	2.02×10^{-3}
1,3-Butadiene	2.00×10^{-3}	2.09×10^{-1}
Benzene	3.00×10^{-2}	1.04×10^{-1}
MTBE	3.00×10^0	7.57×10^{-4}
MMA	7.00×10^{-1}	1.27×10^{-4}
Tetrahydrofuran	2.00×10^0	1.46×10^{-4}
n-Hexane	7.00×10^{-1}	1.35×10^{-3}
Styrene	1.00×10^0	5.38×10^{-4}
Cyclohexane	6.00×10^0	8.66×10^{-5}
Naphthalene	3.00×10^{-3}	6.16×10^{-2}
2-Hexanone	3.00×10^{-2}	6.53×10^{-3}
Vinylchloride	1.00×10^{-1}	1.11×10^{-3}
1,4-Dioxane	3.00×10^{-2}	2.88×10^{-3}
1,2-Dichloropropane	4.00×10^{-3}	7.30×10^{-2}
Trichloroethylene	2.00×10^{-3}	3.55×10^{-2}
1,1-Dichloroethylene	2.00×10^{-1}	3.33×10^{-5}
Dichloromethane	6.00×10^{-1}	4.56×10^{-4}
Methyl bromide	5.00×10^{-3}	4.48×10^{-2}
Perchloroethylene	4.00×10^{-2}	3.14×10^{-3}
1,4-Dicl-benzene	8.00×10^{-1}	6.24×10^{-6}
1,2-Dibromoethane	9.00×10^{-3}	9.39×10^{-4}
Carbon tetrachloride	1.00×10^{-1}	7.35×10^{-3}
Methyl isobutyl ketone	3.00×10^0	5.00×10^{-5}
HI		6.20×10^{-1}

4. Conclusions

In this study, 113 VOCs and ozone were measured in an industrial area in Jinshan District, Shanghai, for 43 days. Days on which the hourly ozone concentration exceeded $200 \mu\text{g}/\text{m}^3$ were classified as polluted days. The highest hourly ozone concentration reached $291 \mu\text{g}/\text{m}^3$ on a polluted day. The average concentration of VOCs was 47.33 ppb during the observation period. The ranking of VOC concentrations was alkanes > OVOCs

> alkenes > aromatics > halogenated hydrocarbons > acetylene. Alkenes were the predominant components that contributed to the OFP, while the greatest contributor to the SOAFP were aromatics. The diurnal variation in VOCs showed two peaks and one valley, indicating that typical VOCs had an accumulation phenomenon in the early morning. Six sources were identified by PMF, including combustion emissions, industrial processes, LPG, solvent usage, vehicle exhaust, and surface coatings. Among them, the big contributors are industrial processes (36.62%), vehicle exhaust (31.56%), and LPG (15.54%). And among the contributions of the OFP, vehicle exhaust is the largest (38.2%), followed by LPG (24%), and industrial process is in third place (17.3%). Therefore, vehicle emissions make an important contribution to the formation of local ozone and should be emphasized for control. The results of a PSCF analysis showed that the potential sources of pollutants were mainly in the west in August and in the southeast in September. In addition to focusing on regional linkages of the surrounding potential source cities, local sources should also be emphasized. The observed hazard indices for VOCs were less than 1, with no non-carcinogenic risk, but 1,3-butadiene, benzene, chloroform, 1,2-dibromoethane, and carbon tetrachloride were higher than 10^{-6} , with a potential carcinogenic risk to the population. It is necessary to take adequate measures to control their emissions.

Author Contributions: Methodology, X.C. and J.Y.; resources, Y.L. and Y.D.; data curation, X.C. and J.Y.; writing—original draft preparation, X.C. and J.Y.; writing—review and editing, X.C. and L.D.; visualization, J.Y.; supervision, L.D., M.Z. and F.Z.; project administration, L.D., Y.L. and Y.D.; funding acquisition, L.D. and F.Z. All authors have read and agreed to the published version of the manuscript.

Funding: This work was supported by the National Natural Science Foundation of China (Grant Nos. 21906055, 42305098) and the Key Research and Development Projects of Shanghai Science and Technology Commission, China (No. 20dz1204000).

Institutional Review Board Statement: Not applicable.

Informed Consent Statement: Not applicable.

Data Availability Statement: The data presented in this study are available upon request from the corresponding author. The data are not publicly available due to privacy.

Conflicts of Interest: The authors declare no conflicts of interest. Mengfei Zhao is employee of Zhejiang Environmental Technology Co., Ltd. The paper reflects the views of the scientists, and not the company.

References

1. Baudic, A.; Gros, V.; Sauvage, S.; Locoge, N.; Sanchez, O.; Sarda-Estève, R.; Kalogridis, C.; Petit, J.-E.; Bonnair, N.; Baisnée, D.; et al. Seasonal variability and source apportionment of volatile organic compounds (VOCs) in the Paris megacity (France). *Atmos. Chem. Phys.* **2016**, *16*, 11961–11989. [[CrossRef](#)]
2. Sahu, L.K.; Tripathi, N.; Yadav, R. Contribution of biogenic and photochemical sources to ambient VOCs during winter to summer transition at a semi-arid urban site in India. *Environ. Pollut.* **2017**, *229*, 595–606. [[CrossRef](#)] [[PubMed](#)]
3. Zhang, Y.; Wang, X.; Zhang, Z.; Lü, S.; Huang, Z.; Li, L. Sources of C2–C4 alkenes, the most important ozone nonmethane hydrocarbon precursors in the Pearl River Delta region. *Sci. Total Environ.* **2015**, *502*, 236–245. [[CrossRef](#)] [[PubMed](#)]
4. Atkinson, R. Atmospheric chemistry of VOCs and NOx. *Atmos. Environ.* **2013**, *34*, 2063–2101. [[CrossRef](#)]
5. Carlier, P.; Hannachi, H.; Mouvier, G. The chemistry of carbonyl compounds in the atmosphere—A review. *Atmos. Environ.* **1986**, *20*, 2079–2099. [[CrossRef](#)]
6. Yu, S.; Wang, S.; Xu, R.; Zhang, D.; Zhang, M.; Su, F.; Zhang, R.; Wang, L. Measurement report: Intra-, inter-annual variability and source apportionment of VOCs during 2018–2020 in Zhengzhou, Central China. *Atmos. Chem. Phys. Discuss.* **2022**, *22*, 1–46.
7. Li, K.; Li, J.; Tong, S.; Wang, W.; Huang, R.J.; Ge, M. Characteristics of wintertime VOCs in suburban and urban Beijing: Concentrations, emission ratios, and festival effects. *Atmos. Chem. Phys.* **2019**, *19*, 8021–8036. [[CrossRef](#)]
8. Li, C.; Liu, Y.; Cheng, B.; Zhang, Y.; Liu, X.; Qu, Y.; An, J.; Kong, L.; Zhang, Y.; Zhang, C.; et al. A comprehensive investigation on volatile organic compounds (VOCs) in 2018 in Beijing, China: Characteristics, sources and behaviours in response to O₃ formation. *Sci. Total Environ.* **2022**, *806*, 150247. [[CrossRef](#)]
9. Tan, Y.; Wang, T. What caused ozone pollution during the 2022 Shanghai lockdown? Insights from ground and satellite observations. *EGUosphere* **2022**, *2022*, 1–21. [[CrossRef](#)]

10. Qi, J.; Mo, Z.; Yuan, B.; Huang, S.; Huangfu, Y.; Wang, Z.; Li, X.; Yang, S.; Wang, W.; Zhao, Y.; et al. An observation approach in evaluation of ozone production to precursor changes during the COVID-19 lockdown. *Atmos. Environ.* **2021**, *262*, 118618. [[CrossRef](#)]
11. Hajizadeh, Y.; Teiri, H.; Nazmara, S.; Parseh, I. Environmental and biological monitoring of exposures to VOCs in a petrochemical complex in Iran. *Environ. Sci. Pollut. Control Ser.* **2018**, *25*, 6656–6667. [[CrossRef](#)] [[PubMed](#)]
12. Liu, Y.; Kong, L.; Liu, X.; Zhang, Y.; Li, C.; Zhang, Y.; Zhang, C.; Qu, Y.; An, J.; Ma, D.; et al. Characteristics, secondary transformation, and health risk assessment of ambient volatile organic compounds (VOCs) in urban Beijing, China. *Atmospheric Pollut. Res.* **2021**, *12*, 33–46. [[CrossRef](#)]
13. Geng, F.; Tie, X.; Xu, J.; Zhou, G.; Peng, L.; Gao, W.; Tang, X.; Zhao, C. Characterizations of ozone, NO_x, and VOCs measured in Shanghai, China. *Atmos. Environ.* **2008**, *42*, 6873–6883. [[CrossRef](#)]
14. Tie, X.; Geng, F.; Peng, L.; Gao, W.; Zhao, C. Measurement and modeling of O₃ variability in Shanghai, China: Application of the WRF-Chem model. *Atmos. Environ.* **2009**, *43*, 4289–4302. [[CrossRef](#)]
15. Cai, C.; Geng, F.; Tie, X.; Yu, Q.; An, J. Characteristics and source apportionment of VOCs measured in Shanghai, China. *Atmos. Environ.* **2010**, *44*, 5005–5014. [[CrossRef](#)]
16. Gao, W.; Tie, X.; Xu, J.; Huang, R.; Mao, X.; Zhou, G.; Chang, L. Long-term trend of O₃ in a mega City (Shanghai), China: Characteristics, causes, and interactions with precursors. *Sci. Total Environ.* **2017**, *603–604*, 425–433. [[CrossRef](#)] [[PubMed](#)]
17. Niu, Y.; Yan, Y.; Xing, Y.; Duan, X.; Yue, K.; Dong, J.; Hu, D.; Wang, Y.; Peng, L. Analyzing ozone formation sensitivity in a typical industrial city in China: Implications for effective source control in the chemical transition regime. *Sci. Total Environ.* **2024**, *919*, 170559. [[CrossRef](#)] [[PubMed](#)]
18. Carter, W.P.L. Updated maximum incremental reactivity scale and hydrocarbon bin reactivities for regulatory applications. *Calif. Air Resour. Board Contract* **2009**, 339, 2009.
19. Grosjean, D. In situ organic aerosol formation during a smog episode: Estimated production and chemical functionality. *Atmos. Environ.* **1992**, *26*, 53–963.
20. Grosjean, D.; Seinfeld, J. Parameterization of the formation potential of secondary organic aerosols. *Atmos. Environ.* **1992**, *23*, 1733–1747. [[CrossRef](#)]
21. Liu, B.; Liang, D.; Yang, J.; Dai, Q.; Bi, X.; Feng, Y.; Yuan, J.; Xiao, Z.; Zhang, Y.; Xu, H. Characterization and source apportionment of volatile organic compounds based on 1-year of observational data in Tianjin, China. *Environ. Pollut.* **2016**, *218*, 757–769. [[CrossRef](#)]
22. Song, M.; Li, L.; Yang, S.; Yu, X.; Zhou, S.; Yang, Y.; Chen, S.; Dong, H.; Liao, K.; Chen, Q.; et al. Spatiotemporal variation, sources, and secondary transformation potential of volatile organic compounds in Xi'an, China. *Atmos. Chem. Phys.* **2021**, *21*, 4939–4958. [[CrossRef](#)]
23. Zhang, C.; Liu, X.; Zhang, Y.; Tan, Q.; Feng, M.; Qu, Y.; An, J.; Deng, Y.; Zhai, Y.; Wang, Z.; et al. Characteristics, source apportionment and chemical conversions of VOCs based on a comprehensive summer observation experiment in Beijing. *Atmospheric Pollut. Res.* **2021**, *12*, 230–241. [[CrossRef](#)]
24. Zhang, K.; Zhou, L.; Fu, Q.; Yan, L.; Bian, Q.; Wang, D.; Xiu, G. Vertical Distribution of Ozone over Shanghai during Late Spring: A Balloon-Borne Observation. *Atmos. Environ.* **2019**, *208*, 48–60. [[CrossRef](#)]
25. Zeng, P.; Huang, X.; Yan, M.; Zheng, Z.; Qiu, Z.; Yun, L.; Lin, C.; Zhang, L. Ambient Ozone and Fine Particular Matter Pollution in a Megacity in South China: Trends, Concurrent Pollution, and Health Risk Assessment. *Atmosphere* **2023**, *14*, 1806. [[CrossRef](#)]
26. Hui, L.; Liu, X.; Tan, Q.; Feng, M.; An, J.; Qu, Y.; Zhang, Y.; Deng, Y.; Zhai, R.; Wang, Z. VOC characteristics, chemical reactivity and sources in urban Wuhan, central China. *Atmos. Environ.* **2020**, *224*, 117340. [[CrossRef](#)]
27. Paatero, P. Least squares formulation of robust non-negative factor analysis. *Chemometr. Intell. Lab. Syst.* **1997**, *37*, 23–35. [[CrossRef](#)]
28. Bon, D.M.; Ulbrich, I.M.; Gouw, J.A.de.; Warneke, C.; Kuster, W.C.; Alexander, M.L.; Baker, A.; Beyersdorf, A.J.; Blake, D.; Fall, R.; et al. Measurements of volatile organic compounds at a suburban ground site (T1) in Mexico City during the MILAGRO 2006 campaign: Measurement comparison, emission ratios, and source attribution. *Atmos. Chem. Phys.* **2011**, *11*, 2399–2421. [[CrossRef](#)]
29. McCarthy, M.C.; Aklilu, Y.-A.; Brown, S.G.; Lyder, D.A. Source apportionment of volatile organic compounds measured in Edmonton, Alberta. *Atmos. Environ.* **2013**, *81*, 504–516. [[CrossRef](#)]
30. Colman Lerner, J.; Sanchez, E.; Sambeth, J.; Porta, A. Characterization and health risk assessment of VOCs in occupational environments in Buenos Aires, Argentina. *Atmos. Environ.* **2012**, *55*, 440–447. [[CrossRef](#)]
31. Hao, R.; Sun, J.; Liu, R.; Zhao, H.; Yao, Z.; Wang, H.; Hao, Z. Emission characteristics, environmental impact, and health risk assessment of volatile organic compounds (VOCs) during manicure processes. *Sci. Total Environ.* **2024**, *906*, 167464. [[CrossRef](#)]
32. Shao, P.; An, J.; Xin, J.; Wu, F.; Wang, J.; Ji, D.; Wang, Y. Source apportionment of VOCs and the contribution to photochemical ozone formation during summer in the typical industrial area in the Yangtze River Delta, China. *Atmos Res.* **2016**, *176–177*, 64–74. [[CrossRef](#)]
33. Li, J.; Zhai, C.; Yu, J.; Liu, R.; Li, Y.; Zeng, L.; Xie, S. Spatiotemporal variations of ambient volatile organic compounds and their sources in Chongqing, a mountainous megacity in China. *Sci. Total Environ.* **2018**, *627*, 1442–1452. [[CrossRef](#)] [[PubMed](#)]
34. Li, B.; Ho, S.S.H.; Gong, S.; Ni, J.; Li, H.; Han, L.; Yang, Y.; Qi, Y.; Zhao, D. Characterization of VOCs and their related atmospheric processes in a central Chinese city during severe ozone pollution periods. *Atmos. Chem. Phys.* **2019**, *19*, 617–638. [[CrossRef](#)]

35. Hoshi, J.-y.; Amano, S.; Sasaki, Y.; Korenaga, T. Investigation and estimation of emission sources of 54 volatile organic compounds in ambient air in Tokyo. *Atmos. Environ.* **2008**, *42*, 2383–2393. [[CrossRef](#)]
36. Zhang, Y.; Li, R.; Fu, H.; Zhou, D.; Chen, J. Observation and analysis of atmospheric volatile organic compounds in a typical petrochemical area in Yangtze River Delta, China. *J. Environ. Sci.* **2018**, *71*, 233–248. [[CrossRef](#)] [[PubMed](#)]
37. Lin, L.; Cheng, Y.; Cao, L.; Yu, G.; Huang, X. The characterization and source apportionment of VOCs in Shenzhen during ozone polluted period. *China Environ. Sci.* **2021**, *41*, 3484–3492.
38. Zheng, H.; Kong, S.; Yan, Y.; Chen, N.; Yao, L.; Liu, X.; Wu, F.; Cheng, Y.; Niu, Z.; Zheng, S.; et al. Compositions, sources and health risks of ambient volatile organic compounds (VOCs) at a petrochemical industrial park along the Yangtze River. *Sci. Total Environ.* **2020**, *703*, 135505. [[CrossRef](#)]
39. Liu, Y.; Shao, M.; Fu, L.; Lu, S.; Zeng, L.; Tang, D. Source profiles of volatile organic compounds (VOCs) measured in China: Part I. *Atmos. Environ.* **2008**, *42*, 6247–6260. [[CrossRef](#)]
40. Wu, R.; Li, J.; Hao, Y.; Li, Y.; Zeng, L.; Xie, S. Evolution process and sources of ambient volatile organic compounds during a severe haze event in Beijing, China. *Sci. Total Environ.* **2016**, *560–561*, 62–72. [[CrossRef](#)] [[PubMed](#)]
41. Wei, W.; Lv, Z.; Yang, G.; Cheng, S.; Li, Y.; Wang, L. VOCs emission rate estimate for complicated industrial area source using an inverse-dispersion calculation method: A case study on a petroleum refinery in Northern China. *Environ. Pollut.* **2016**, *218*, 681–688. [[CrossRef](#)] [[PubMed](#)]
42. Li, L.; Zhang, D.; Hu, W.; Yang, Y.; Zhang, S.; Yuan, R.; Lv, P.; Zhang, W.; Zhang, Y.; Zhang, Y. Improving VOC control strategies in industrial parks based on emission behavior, environmental effects, and health risks: A case study through atmospheric measurement and emission inventory. *Sci. Total Environ.* **2023**, *865*, 161235. [[CrossRef](#)] [[PubMed](#)]
43. Maji, S.; Beig, G.; Yadav, R. Winter VOCs and OVOCs measured with PTR-MS at an urban site of India: Role of emissions, meteorology and photochemical sources. *Environ. Pollut.* **2020**, *258*, 113651. [[CrossRef](#)] [[PubMed](#)]
44. Oku, H.; Inafuku, M.; Takamine, T.; Nagamine, N.; Saitoh, S.; Fukuta, M. Temperature threshold of isoprene emission from tropical trees, *Ficus virgata* and *Ficus septica*. *Chemosphere* **2014**, *95*, 268–273. [[CrossRef](#)]
45. Buzcu, B.; Fraser, M.P. Source identification and apportionment of volatile organic compounds in Houston, TX. *Atmos. Environ.* **2006**, *40*, 2385–2400. [[CrossRef](#)]
46. Russo, R.S.; Zhou, Y.; White, M.L.; Mao, H.; Talbot, R.; Sive, B.C. Multi-year (2004–2008) record of nonmethane hydrocarbons and halocarbons in New England: Seasonal variations and regional sources. *Atmos. Chem. Phys.* **2010**, *10*, 4909–4929. [[CrossRef](#)]
47. Zheng, H.; Kong, S.; Xing, X.; Mao, Y.; Hu, T.; Ding, Y.; Li, G.; Liu, D.; Li, S.; Qi, S. Monitoring of volatile organic compounds (VOCs) from an oil and gas station in northwest China for 1 year. *Atmos. Chem. Phys.* **2018**, *18*, 4567–4595. [[CrossRef](#)]
48. Nelson, P.F.; Quigley, S.M. The m,p-xylenes:ethylbenzene ratio. A technique for estimating hydrocarbon age in ambient atmospheres. *Atmos. Environ.* **1983**, *17*, 659–662. [[CrossRef](#)]
49. Vardoulakis, S.; Solazzo, E.; Lumbrellas, J. Intra-urban and street scale variability of BTEX, NO₂ and O₃ in Birmingham, UK: Implications for exposure assessment. *Atmos. Environ.* **2011**, *45*, 5069–5078. [[CrossRef](#)]
50. Hui, L.; Liu, X.; Tan, Q.; Feng, M.; An, J.; Qu, Y.; Zhang, Y.; Cheng, N. VOC characteristics, sources and contributions to SOA formation during haze events in Wuhan, Central China. *Sci. Total Environ.* **2019**, *650*, 2624–2639. [[CrossRef](#)]
51. Hui, L.; Liu, X.; Tan, Q.; Feng, M.; An, J.; Qu, Y.; Zhang, Y.; Jiang, M. Characteristics, source apportionment and contribution of VOCs to ozone formation in Wuhan, Central China. *Atmos. Environ.* **2018**, *192*, 55–71. [[CrossRef](#)]
52. Zheng, J.; Yu, Y.; Mo, Z.; Zhang, Z.; Wang, X.; Yin, S.; Peng, K.; Yang, Y.; Feng, X.; Cai, H. Industrial sector-based volatile organic compound (VOC) source profiles measured in manufacturing facilities in the Pearl River Delta, China. *Sci. Total Environ.* **2013**, *456–457*, 127–136. [[CrossRef](#)] [[PubMed](#)]
53. Song, M.; Liu, X.; Zhang, Y.; Shao, M.; Lu, K.; Tan, Q.; Feng, M.; Qu, Y. Sources and abatement mechanisms of VOCs in southern China. *Atmos. Environ.* **2019**, *201*, 28–40. [[CrossRef](#)]
54. Ling, Z.H.; Guo, H.; Cheng, H.R.; Yu, Y.F. Sources of ambient volatile organic compounds and their contributions to photochemical ozone formation at a site in the Pearl River Delta, southern China. *Environ. Pollut.* **2011**, *159*, 2310–2319. [[CrossRef](#)]
55. Song, C.; Liu, B.; Dai, Q.; Li, H.; Mao, H. Temperature dependence and source apportionment of volatile organic compounds (VOCs) at an urban site on the north China plain. *Atmos. Environ.* **2019**, *207*, 167–181. [[CrossRef](#)]
56. Yao, Z.; Shen, X.; Ye, Y.; Cao, X.; Jiang, X.; Zhang, Y.; He, K. On-road emission characteristics of VOCs from diesel trucks in Beijing, China. *Atmos. Environ.* **2015**, *103*, 87–93. [[CrossRef](#)]
57. Xiong, Y.; Zhou, J.; Xing, Z.; Du, K. Optimization of a volatile organic compound control strategy in an oil industry center in Canada by evaluating ozone and secondary organic aerosol formation potential. *Environ. Res.* **2020**, *191*, 110217. [[CrossRef](#)]
58. Huang, A.; Yin, S.; Yuan, M.; Xu, Y.; Yu, S.; Zhang, D.; Lu, X.; Zhang, R. Characteristics, source analysis and chemical reactivity of ambient VOCs in a heavily polluted city of central China. *Atmospheric Pollut. Res.* **2022**, *13*, 101390. [[CrossRef](#)]
59. Zhou, J.; You, Y.; Bai, Z.; Hu, Y.; Zhang, J.; Zhang, N. Health risk assessment of personal inhalation exposure to volatile organic compounds in Tianjin, China. *Sci. Total Environ.* **2011**, *409*, 452–459. [[CrossRef](#)]

Disclaimer/Publisher’s Note: The statements, opinions and data contained in all publications are solely those of the individual author(s) and contributor(s) and not of MDPI and/or the editor(s). MDPI and/or the editor(s) disclaim responsibility for any injury to people or property resulting from any ideas, methods, instructions or products referred to in the content.